Brief Communication

MOLECULAR METABOLISM

Altered pancreatic islet morphology and function in SGLT1 knockout mice on a glucose-deficient, fat-enriched diet

Markus Mühlemann [1,5], Daniela Zdzieblo [1,*,5], Alexandra Friedrich [2], Constantin Berger [1], Christoph Otto [3], Heike Walles [1,4], Hermann Koepsell [2,6], Marco Metzger [1,4,6]

ABSTRACT

Objectives: Glycemic control by medical treatment represents one therapeutic strategy for diabetic patients. The Na+-D-glucose cotransporter 1 (SGLT1) is currently of high interest in this context. SGLT1 is known to mediate glucose absorption and incretin secretion in the small intestine. Recently, inhibition of SGLT1 function was shown to improve postprandial hyperglycemia. In view of the lately demonstrated SGLT1 expression in pancreatic islets, we investigated if loss of SGLT1 affects islet morphology and function.

Methods: Effects associated with the loss of SGLT1 on pancreatic islet (cyto) morphology and function were investigated by analyzing islets of a SGLT1 knockout mouse model, that were fed a glucose-deficient, fat-enriched diet (SGLT1$^{-/-}$-GDFE) to circumvent the glucose-galactose malabsorption syndrome. To distinguish diet- and Sglt1$^{-/-}$-dependent effects, wildtype mice on either standard chow (WT-SC) or the glucose-free, fat-enriched diet (WT-GDFE) were used as controls. Feeding a glucose-deficient, fat-enriched diet further required the analysis of intestinal SGLT1 expression and function under diet-conditions.

Results: Consistent with literature, our data provide evidence that small intestinal SGLT1 mRNA expression and function is regulated by nutrition. In contrast, pancreatic SGLT1 mRNA levels were not affected by the applied diet, suggesting different regulatory mechanisms for SGLT1 in diverse tissues. Morphological changes such as increased islet sizes and cell numbers associated with changes in proliferation and apoptosis and alterations of the β- and α-cell population are specifically observed for pancreatic islets of SGLT1$^{-/-}$-GDFE mice. Glucose stimulation revealed no insulin response in SGLT1$^{-/-}$-GDFE mice while WT-GDFE mice displayed only a minor increase of blood insulin. Irregular glucagon responses were observed for both, SGLT1$^{-/-}$-GDFE and WT-GDFE mice. Further, both animal groups showed a sustained release of GLP-1 compared to WT-SC controls.

Conclusion: Loss or impairment of SGLT1 results in abnormal pancreatic islet (cyto)morphology and disturbed islet function regarding the insulin or glucagon release capacity from β- or α-cells, respectively. Consequently, our findings propose a new, additional role for SGLT1 maintaining proper islet structure and function.

© 2018 The Authors. Published by Elsevier GmbH. This is an open access article under the CC BY-NC-ND license (http://creativecommons.org/licenses/by-nc-nd/4.0/).

Keywords Glucose transporter SGLT1; Pancreatic islet cytomorphology; Pancreatic islet function; β-cell; α-cell

1. INTRODUCTION

The Na$^+$-D-glucose cotransporter 1 (SGLT1) is encoded by the *Slc5a1* gene predominantly expressed in the small intestine [1,2]. In addition, SGLT1 expression was also shown in various other tissues such as kidney, lung, liver, heart, brain, uterus, and pancreas [1–6]; with the exception of the small intestine, kidney, and uterus, tissue-specific function is widely unknown.

The classical role of small intestinal SGLT1 is secondary, active Na$^+$-D-glucose cotransport across the apical membrane, which is rate-limiting for intestinal glucose absorption from food [2,7,8]. Additionally, along with the glucose transport, incretins such as glucagon-like peptide 1 (GLP-1) are secreted [9–11]. Incretins, especially GLP-1, act on pancreatic islets contributing to the regulation of insulin secretion from β-cells [9–11]. Functional impairments are seen when SGLT1 is abrogated. Humans carrying mutations in SGLT1 display a diminished capacity for small intestinal glucose transport [12]. Further, aberrant glucose-stimulated insulin or GLP-1 responses were reported for SGLT1 inhibition or knockout (SGLT1$^{-/-}$) mice [7,8,13–15]. Consequently, SGLT1 plays a crucial role in the regulation of blood glucose homeostasis.

[1]Chair Tissue Engineering and Regenerative Medicine, University Hospital Würzburg, 97070, Würzburg, Germany [2]Department of Molecular Plant Physiology and Biophysics, Julius-von-Sachs-Institute, University of Würzburg, 97070, Würzburg, Germany [3]Department of General Visceral Vascular and Pediatric Surgery, University Hospital Würzburg, 97070, Würzburg, Germany [4]Translational Center Regenerative Therapies (TLC-RT), Fraunhofer Institute for Silicate Research ISC, 97070, Würzburg, Germany

[5] These two authors have contributed equally to this work and are sharing the first authorship.
[6] These two authors have contributed equally to this work and are sharing the last authorship.

*Corresponding author. Fax: +49 931 31 81068. E-mail: daniela.zdzieblo@uni-wuerzburg.de (D. Zdzieblo).

Received April 20, 2018 • Revision received May 8, 2018 • Accepted May 15, 2018 • Available online 23 May 2018

https://doi.org/10.1016/j.molmet.2018.05.011

 © 2018 The Authors. Published by Elsevier GmbH. This is an open access article under the CC BY-NC-ND license (http://creativecommons.org/licenses/by-nc-nd/4.0/).

Maintaining blood glucose homeostasis is of high importance for type 2 diabetes (T2D) patients. T2D is a widespread disease with severe long-term associated complications that is characterized by hyperglycemia, decreased insulin sensitivity of target tissues, and decreased insulin secretion of pancreatic β-cells. Pharmacological agents regulating blood glucose levels under diabetic conditions represent a promising treatment strategy. After successful establishment of Na^+-D-glucose cotransporter 2 (SGLT2) inhibitors blocking renal glucose reabsorption, inhibitors of SGLT1 that block small intestinal glucose absorption have been proposed recently as an additional therapeutic intervention strategy [14–16]. Preclinical studies and first clinical trials show that the application of SGLT1 inhibitors, alone or in combination with SGLT2 inhibition, improve postprandial hyperglycemia in diabetic patients [15–18]. However, effects of long-term treatment have not been evaluated in detail. In addition, there is considerable uncertainty concerning potential side effects. Diarrhea, abdominal pain, and flatulence have been reported [16], but there is some disagreement whether these effects may be moderate if complete blockage of SGLT1 is avoided [19]. Studies in humans or mice kept on a standard diet exhibiting defect mutations in SGLT1 similarly demonstrated intestinal malabsorption of glucose and galactose associated with diarrhea and metabolic acidosis [7,8,12,20]. Further, endometrial side effects were shown for SGLT1 knockout mice [5]. Knowledge about adverse events in other SGLT1 expressing tissues is largely missing.

In view of the recently reported SGLT1 expression in pancreatic islet cells [3,6] together with the atypical insulin responses reported for $SGLT1^{-/-}$ mice [7,8] and the current interest in pharmacological SGLT1 inhibition, the aim of our work was to investigate possible side effects on pancreatic islets when SGLT1 is lost. This may also contribute to a better understanding of a pancreas-specific SGLT1 function.

2. METHODS

2.1. Animal handling

Animal research was performed according to German law and institutional guidelines approved by the Ethics Committee of the District of Unterfranken, Würzburg, Germany (approval number: 55.2-2531.01-45/14). Mice were housed with free access to food and water *ad libitum* at 12 h light and dark cycles. Wild type mice and $SGLT1^{-/-}$ mice on C57BL6/J background were fed with two different but equicaloric diets both containing about 13 MJ kg^{-1} as described [7]. Standard chow (SC) was obtained from Altromin (Lage, Germany; #1320) containing 36.4% starch, 19% protein, 4.9% fiber, 4.7% mono- and disaccharides, 3.3% fat, minerals and vitamins. The glucose-deficient, fat-enriched diet (GDFE) in which energy content was supplemented by increased fat and protein was composed of 33.8% protein, 30.7% fiber, 20.5% fat, minerals and vitamins (Altromin, Lage, Germany #C-1073). Three animal groups were compared: wild type mice fed with SC (WT-SC), wild type or $SGLT1^{-/-}$ mice fed with GDFE (WT-GDFE or $SGLT1^{-/-}$-GDFE mice). Diets were applied directly after weaning, and analyses were performed in 12 - 14 week old animals.

2.2. Oral glucose tolerance test (OGTT) and *in vitro* glucose measurement

Animals were deprived of food 12 h prior to administration of D-glucose (6 mg/g body weight). PBS served as control. Blood samples were taken 5 or 60 min after bolus from the left heart of sacrificed animals followed by dilution in citrate buffer (pH 4.5) substituted with 100 μmol/L dipeptidyl peptidase (DPP)-IV inhibitor (Merck Millipore, Darmstadt, Germany). Plasma insulin or GLP-1 values were analyzed using the insulin ultrasensitive mouse ELISA (80-INSMSU-E01, Alpco, Salem, USA), the total GLP-1 ELISA (EZGLP1T-36K, Merck Millipore, Darmstadt, Germany) or the Glucagon ELISA (10-1281-01, Mercodia, Uppsala, Sweden). For blood glucose determination the Glucose Colorimetric Assay Kit (10009582, Cayman Chemicals, Ann Arbor, U.S.A.) was used following manufacturer's instructions.

2.3. Islet isolation and glucose-stimulated insulin secretion (GSIS)

Pancreatic islets were isolated as described with modifications [21,22]. Briefly, islets were obtained by perfusion of pancreata with Collagenase P (1.2 mg/ml, Roche, Basel, Switzerland) dissolved in 2 ml RPMI 1640 medium through the common bile duct followed by organ isolation and enzymatic dissociation at 37 °C. After washing, islets and the exocrine pancreatic tissue were separated by Ficoll Paque (GE Healthcare, Chicago, USA) gradient centrifugation followed by hand-picking of islets. Prior to glucose stimulation, islets were cultured at 37 °C for 90 min in RPMI 1640, 10% FCS, 1x GlutaMax, 20 mM HEPES sodium salt solution and 1x Penicillin-Streptomycin followed by 30 min incubation in 3.3 mM D-glucose dissolved in Krebs buffer working solution (137 mM NaCl, 4.7 mM KCl, 1.2 mM KH_2PO_4, 1.2 mM $MgSO_4$, 2.5 mM $CaCl_2$, 25 mM $NaHCO_3$). Afterwards, islets were stimulated in 3.3 mM or 16.7 mM D-glucose solution. After 1 h, supernatants were removed and analyzed for insulin concentration using the ultrasensitive mouse insulin ELISA (Alpco, Salem, USA). DNA content was quantified with the Quant-it dsDNA PicoGreen Kit (Thermo Fisher, Darmstadt, Germany). Stimulation index was calculated by dividing high glucose insulin/DNA ratio by low glucose insulin/DNA ratio.

2.4. Hematoxylin-eosin (H&E) and immunohistological (IHC) analyses

H&E staining's were performed according to a standard protocol. Prior to IHC stainings, sections were rehydrated. Heat-induced epitope retrieval was achieved by 20 min boiling in citrate buffer (pH 6). After permeabilization by Triton X-treatment (0.2%), unspecific binding sites were blocked by incubation in 5% (v/v) donkey serum, 0.5% BSA (w/v) and 0.2% Saponin (w/v) or in 5% BSA only. Primary antibodies were incubated at 4 °C overnight. Next day and after several rounds of washing, sections were incubated with secondary antibodies at room-temperature for 1 h before additional washing steps and mounting in Fluoromount-G containing DAPI. Antibodies are listed in Supplementary Table 1. Analysis was performed using inverse fluorescence (BZ-7000, Keyence, Tokyo, Japan) or confocal microscopy (TCS SP8, Leica Microsystems, Wetzlar, Germany). Quantification of islet size and determination of cell numbers was performed on H&E-stained sections using Image J and the ImageJ Cell Counter plugin (ImageJ, National Institutes of Health, Bethesda, USA). Triglyceride staining was performed using Oil Red O (Sigma Aldrich, Munich, Germany) according to manufacturer's instructions.

2.5. Apoptosis assay

Islets were isolated as described and dissociated into single cell suspensions using 0.05% trypsin-EDTA (v/v) for 5 min at 37 °C. Single cell suspensions were analyzed for apoptotic cell numbers using the fluorochrome-labeled Annexin V apoptosis kit (BioLegend, San Diego, USA) according to manufacturer's instructions and the BD Accuri™ C6 Cytometer (BD Biosciences, Heidelberg, Germany).

2.6. Quantitative (q)RT-PCR

RNA was isolated using the RNeasy Micro or Mini Kit and cDNA was synthesized with the iScript™ cDNA Synthesis Kit (Biorad, Munich,

 © 2018 The Authors. Published by Elsevier GmbH. This is an open access article under the CC BY-NC-ND license (http://creativecommons.org/licenses/by-nc-nd/4.0/).

Germany). qRT-PCR was performed on the CFX96 Touch™ Real-Time PCR Detection System (Biorad) using SsoFast™ EvaGreen® Supermix (Biorad). Gene expression was calculated by the $2^{-\Delta\Delta Ct}$ method with *RPL15* as reference gene. All reactions were performed in duplicates at 60 °C annealing temperature. Primers were applied at 4 pmol/µl. Primer sequences are shown in Supplementary Table 2.

2.7. Statistical analysis

If not otherwise described, data are shown as mean ± standard deviation (SD). Comparing mean values of three or more conditions, significance of differences was analyzed using one-way ANOVA with posthoc Tukey comparison. Significance between two mean values was determined by Student's *t*-test. Statistical analysis was performed with Graph Pad Prism 6.07 (GraphPad Software Inc., La Jolla, USA). $P < 0.05$ was considered statistically significant.

3. RESULTS

3.1. Glucose-deficient, fat-enriched diet impacts small intestinal but not pancreatic SGLT1 mRNA expression

SGLT1 is predominantly expressed in the small intestine; however, protein and/or mRNA of SGLT1 has also been detected in various additional organs including the pancreas [1–3,5,6,23,24]. Consistent with earlier findings [3,6,23], we observed SGLT1 mRNA expression in small intestine (SI), pancreatic islets (PIs), and pancreatic exocrine tissue (EXT) of WT-SC mice (Figure 1). Compared to SI, SGLT1 mRNA expression in PIs or EXT was only 0.23% or 0.28%, respectively (Figure 1A). In addition to tissue-specific transcription [1,2,23], nutrient-dependent regulation was shown for small intestinal SGLT1 mRNA expression [1,25–27]. We observed that SGLT1 mRNA expression in SI of WT-GDFE mice was downregulated by 84.1% compared to WT-SC controls (Figure 1B). In line with the decrease in mRNA expression, also blood glucose levels were significantly reduced in WT-GDFE mice 5 min post glucose administration compared to WT-SC controls (Supplementary Fig. 1). In contrast to the intestine, SGLT1 mRNA expression levels in PIs and EXT of WT mice on SC or GDFE were similar (Figure 1C and D). Of note, there was a huge variation for SGLT1 mRNA expression observed in WT-GDFE PIs and EXT; however, the reason remains elusive (Figure 1C and D). As expected no significant expression of SGLT1 mRNA could be detected in SGLT1$^{-/-}$-GDFE mice (Figure 1B–D). Also, no increase in blood glucose was observed in SGLT1$^{-/-}$-GDFE mice 5 min post glucose administration while all mice displayed comparable blood glucose levels after a 12 h fasting period (Supplementary Fig. 1A–B).

3.2. Pancreatic islets of SGLT1$^{-/-}$-GDFE mice show increased sizes associated with elevated cell numbers, decreased cellular proliferation, and a reduction in apoptotic cells

In the current study, we aimed to investigate if SGLT1 knockout impacts PIs. To this aim, we first investigated morphological aspects of PIs analyzing islet areas in WT-SC, WT-GDFE, and SGLT1$^{-/-}$-GDFE mice (Figure 2 and B; Supplementary Fig. 2). Whereas no significant difference was detected between WT-SC and WT-GDFE mice, a 48% larger compiled islet area was observed in SGLT1$^{-/-}$-GDFE mice compared to WT-GDFE mice. To determine whether the increased, compiled PI area was due to an increase of islet size, we compared islet sizes between WT-SC, WT-GDFE, and SGLT1$^{-/-}$-GDFE mice (Figure 2C). Islet sizes are known to vary from small to large and islet

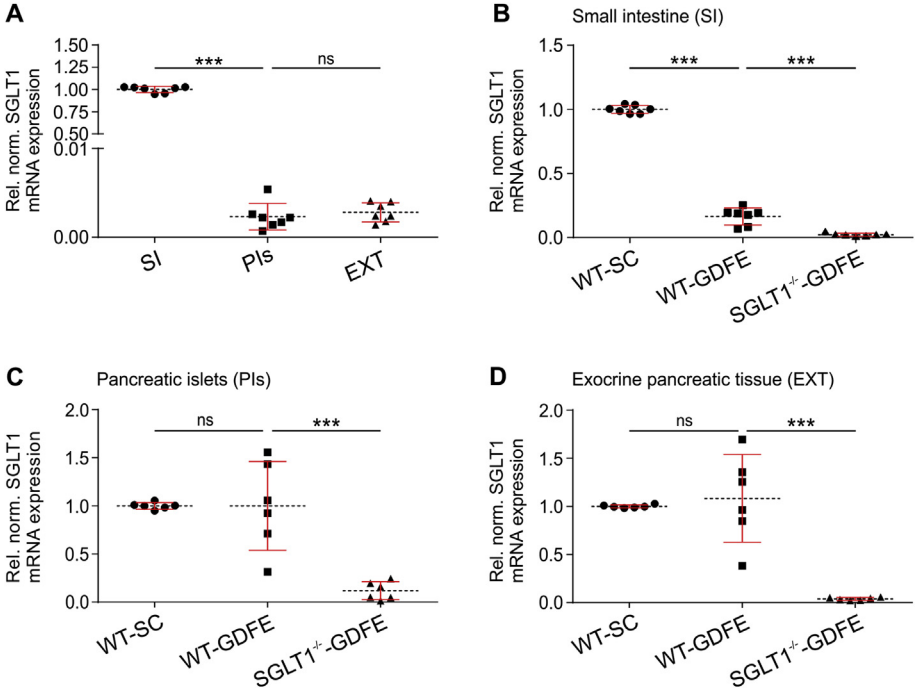

Figure 1: SGLT1 mRNA expression in small intestine (SI), pancreatic islets (PI) and pancreatic exocrine tissue (EXT) isolated from WT-SC, WT-GDFE or SGLT1$^{-/-}$-GDFE mice. SGLT1 mRNA levels were determined by quantitative RT-PCR using the $2^{-\Delta\Delta Ct}$ method with murine *(m)RPL15* as reference gene. **(A)** Comparison of SGLT1 mRNA expression in SI, PIs, and EXT of WT-SC mice. Data are presented relative to SGLT1 mRNA expression in SI and are shown as means ± SD with indication of individual measurements. For calculation, each biological replicate of SI-specific SGLT1 mRNA expression was set to 1. **(B–D)** Comparison of SGLT1 mRNA expression in SI (B), PI (C), or EXT (D) between WT-SC, WT-GDFE, and SGLT1$^{-/-}$-GDFE mice. Data are presented relative to SGLT1 mRNA expression in WT-SC mice and are shown as means ± SD with indication of individual measurements. For calculation, expression in WT-SC mice was set to 1 for each biological replicate. Experiments were performed with female mice ($n = 6$). ***$P < 0.001$, ns = not significant one-way ANOVA with posthoc Tukey test.

 © 2018 The Authors. Published by Elsevier GmbH. This is an open access article under the CC BY-NC-ND license (http://creativecommons.org/licenses/by-nc-nd/4.0/).

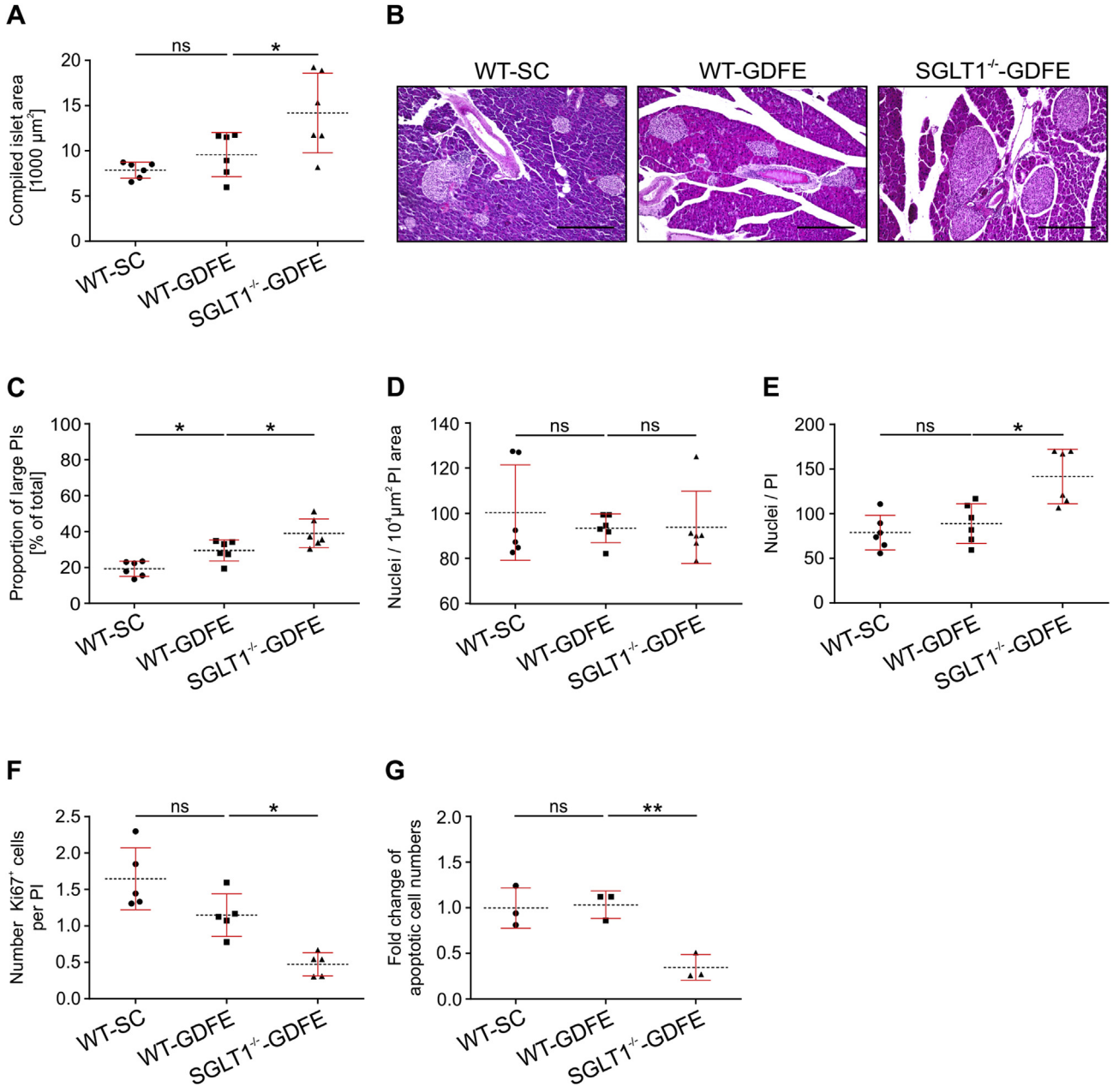

Figure 2: Comparison of compiled islet area, proportion of large islets, cell numbers per pancreatic islets (PIs), PI-specific proliferation, and apoptosis in WT-SC, WT-GDFE, and SGLT1$^{-/-}$-GDFE mice. Data are shown as means ± SD. **(A)** Compiled areas of PIs. Per animal, 4–6 H&E-stained sections from different stacks (see Supplementary Fig. 2) were used for determination of compiled islet areas. Shown are the average compiled areas for each group. Measurements from individual animals and mean values ± SD are shown ($n = 6$). **(B)** Representative microscopic pictures of H&E-stained pancreas sections of WT-SC, WT-GDFE, and SGLT1$^{-/-}$-GDFE mice. Scale bar = 300 µm. **(C)** Proportions of pancreatic islets with areas $> 12 \times 10^3$ µm^2. 4–6 H&E-stained sections per animal were analyzed and the data are presented as in (A) ($n = 6$). **(D)** Cells per islet area. Cell numbers were determined by counting nuclei in 4–6 H&E-stained tissue sections per animal ($n = 6$). The data are presented as in (A). **(E)** Average numbers of cells per PI. Nuclei were counted in 4–6 H&E-stained serial sections. Data are presented as in (A) ($n = 6$). **(F)** Cell proliferation in PIs. Consecutive pancreas sections were double stained with the nuclear stain DAPI and an antibody against the nuclear proliferation marker KI67 (see Supplementary Fig. 3). Graph shows the proportion of KI67$^+$ cells in PIs. Data are presented as in (A) ($n = 5$). **(G)** Comparison of apoptotic cells in isolated PIs stained with Annexin V-FITC/7AAD-PE apoptosis detection kit from BioLegend (San Diego CA, USA). Analysis was performed using flow cytometry (see Supplementary Fig. 4). Numbers of apoptotic cells determined in WT-GDFE or SGLT1$^{-/-}$-GDFE mice are presented relative to numbers obtained for PIs from WT-SC mice. For calculation, numbers obtained for PIs from WT-SC mice were set to 1 for each biological replicate ($n = 3$). All experiments shown in this figure were performed with male mice. *$P < 0.05$, **$P < 0.01$, ns = not significant ANOVA with posthoc Tukey comparison.

size distribution patterns are influenced by physiological or pathological conditions [28]. Dividing the pancreatic islets into small islets comprising areas $<12 \times 10^3$ µm^2 and large islets with areas $>12 \times 10^3$ µm^2, we observed 19% large islets in WT-SC mice, 29% in WT-GDFE mice and 39% in SGLT1$^{-/-}$-GDFE mice (Figure 2C). To investigate whether the increased islet sizes observed for WT-GDFE and SGLT1$^{-/-}$-GDFE mice (Figure 2A) correlated with a change in cellular density, we determined the amount of cell nuclei in pancreatic

 © 2018 The Authors. Published by Elsevier GmbH. This is an open access article under the CC BY-NC-ND license (http://creativecommons.org/licenses/by-nc-nd/4.0/).

islets per area without differentiating between small and large islets. Our data showed no significant differences between all three groups (Figure 2D). In contrast to cellular density but consistent with the larger compiled islet area (Figure 2A), we observed a 60% higher number of cells per islet in SGLT1$^{-/-}$-GDFE compared to WT-GDFE mice whereas cell numbers per islet for WT-SC and WT-GDFE mice were similar (Figure 2E). To further evaluate whether the higher number of islet cells in SGLT1$^{-/-}$-GDFE mice was due to changes in proliferation and/or apoptosis, we first determined the fraction of cells per islet expressing the proliferation marker KI67 [29] without differentiating between islet sizes (Figure 2F; Supplementary Fig. 3). In WT-SC mice, about 1.64 $\pm$ 0.42 KI67^{+} cells per islet were observed. Whereas no diet-dependent effect was detected, the number of KI67^{+} cells in SGLT1$^{-/-}$-GDFE mice (0.47 $\pm$ 0.15) was significantly reduced compared to WT-GDFE mice (1.14 $\pm$ 0.29). We further determined the number of apoptotic cells by flow cytometry analysis. Figure 2G shows fold changes of apoptotic cell numbers of WT-GDFE and SGLT1$^{-/-}$-GDFE mice relative to WT-SC mice. While no difference was observed between WT-SC and WT-GDFE mice, PIs of SGLT1$^{-/-}$-GDFE mice showed 2.3-fold less apoptotic cell numbers compared to WT-GDFE mice (Figure 2G; Supplementary Fig. 4).

3.3. SGLT1 knockout impacts on the β- and α-cell proportion of PIs

To gain deeper insights into pancreatic islet cytomorphology, we next performed double immunohistological (IHC) staining's on pancreas sections of WT-SC, WT-GDFE, and SGLT$^{-/-}$-GDFE mice with antibodies against insulin and glucagon to investigate the two main endocrine cell types within the islet. In all three groups, two phenotypes of islet cytomorphology could be distinguished: a typical cytomorphology with a core of more than 60% β-cells per PI surrounded by a mantle of less than 20% α-cells per PI, and an atypical cytomorphology characterized by a reduction in the β-cell core (<60% of PI) and an increased cluster of α-cells (>20% per PI) (Figure 3A and B). The number of atypical islets was significantly different between WT-SC, WT-GDFE, and SGLT1$^{-/-}$-GDFE mice (Figure 3B). We observed 22.4 $\pm$ 12.1% atypical islets in WT-SC mice, 40.6 $\pm$ 12% in WT-GDFE mice, and 72.2 $\pm$ 12.2% in SGLT1$^{-/-}$-GDFE mice. In Figure 3C and D, the proportion of β- and α-cells per PI without distinguishing between typical and atypical islets is shown. The data indicate similar proportions of β- and α-cells between WT-SC and WT-GDFE mice, whereas SGLT1$^{-/-}$-GDFE mice contained significantly less β- but more α-cells per islet compared to WT-GDFE mice. In contrast, gene expression analysis for insulin and glucagon in isolated PIs, revealed similar mRNA expression levels between WT-GDFE and SGLT$^{-/-}$-GDFE mice compared to WT-SC controls (Supplementary Figs. 5A and B).

3.4. Decreased insulin but unchanged glucagon levels are observed after glucose-stimulation of isolated islets from WT-GDFE and SLGT1$^{-/-}$-GDFE mice

To determine whether the atypical proportion of β- and α-cells in SGLT1$^{-/-}$ islets associates with changes in the secretion of insulin or glucagon, we isolated islets from all three animal groups and measured insulin or glucagon levels after glucose stimulation *in vitro*. We observed a significantly decreased stimulation index for insulin secretion of PIs obtained from WT-GDFE mice compared to WT-SC controls, whereas SGLT1 knockout had no significant effect (Figure 4A). In contrast, glucagon levels were similar between all three groups independent of low or high glucose concentrations (Figure 4B and C). In view of the diminished insulin-secretion capacity of WT-

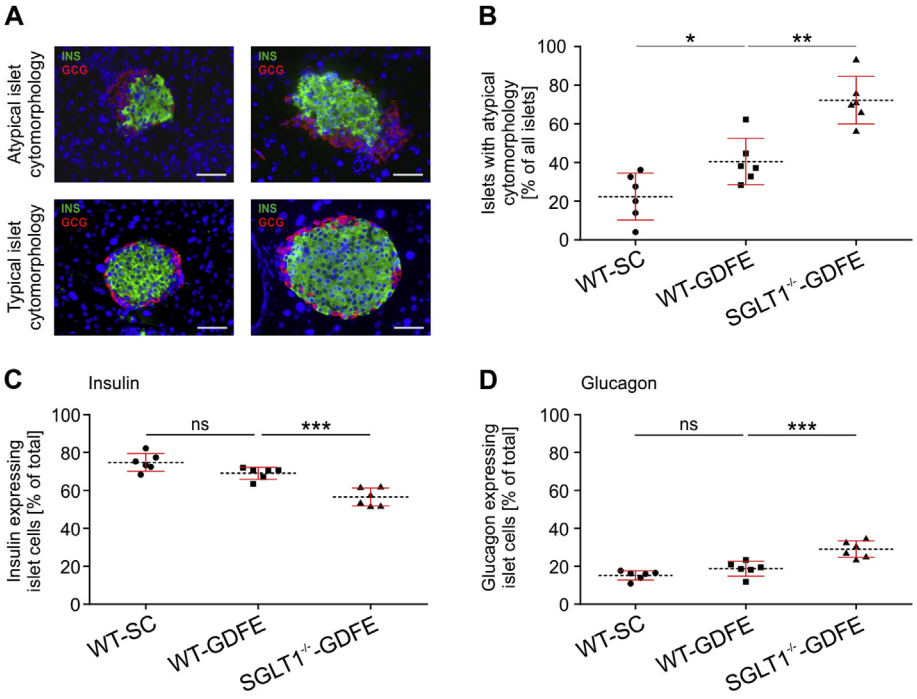

Figure 3: Cytomorphology of pancreatic islets (PIs) from WT-SC, WT-GDFE and SGLT1$^{-/-}$-GDFE mice. Individual measurements of β- and α-cell proportions are indicated as means $\pm$ SD. **(A)** Representative pictures of PIs with atypical and typical cytomorphology. The PIs were stained with antibodies against insulin for β-cells (INS, green), glucagon for α-cells (GCG, red), and DAPI (blue). Scale bar = 100 μm. *B:* Proportion of PIs showing an atypical cytomorphology ($n = 6$). Per male animal, 4–6 sections from different stacks were analyzed. **(C,D)** Proportion of β- (C) or α-cells (D) related to total counted cells per islet ($n = 6$). 4–6 sections of different stacks were analyzed. *$P < 0.05$, **$P < 0.01$, ***$P < 0.001$, ns = not significant ANOVA with posthoc Tukey comparison.

 © 2018 The Authors. Published by Elsevier GmbH. This is an open access article under the CC BY-NC-ND license (http://creativecommons.org/licenses/by-nc-nd/4.0/).

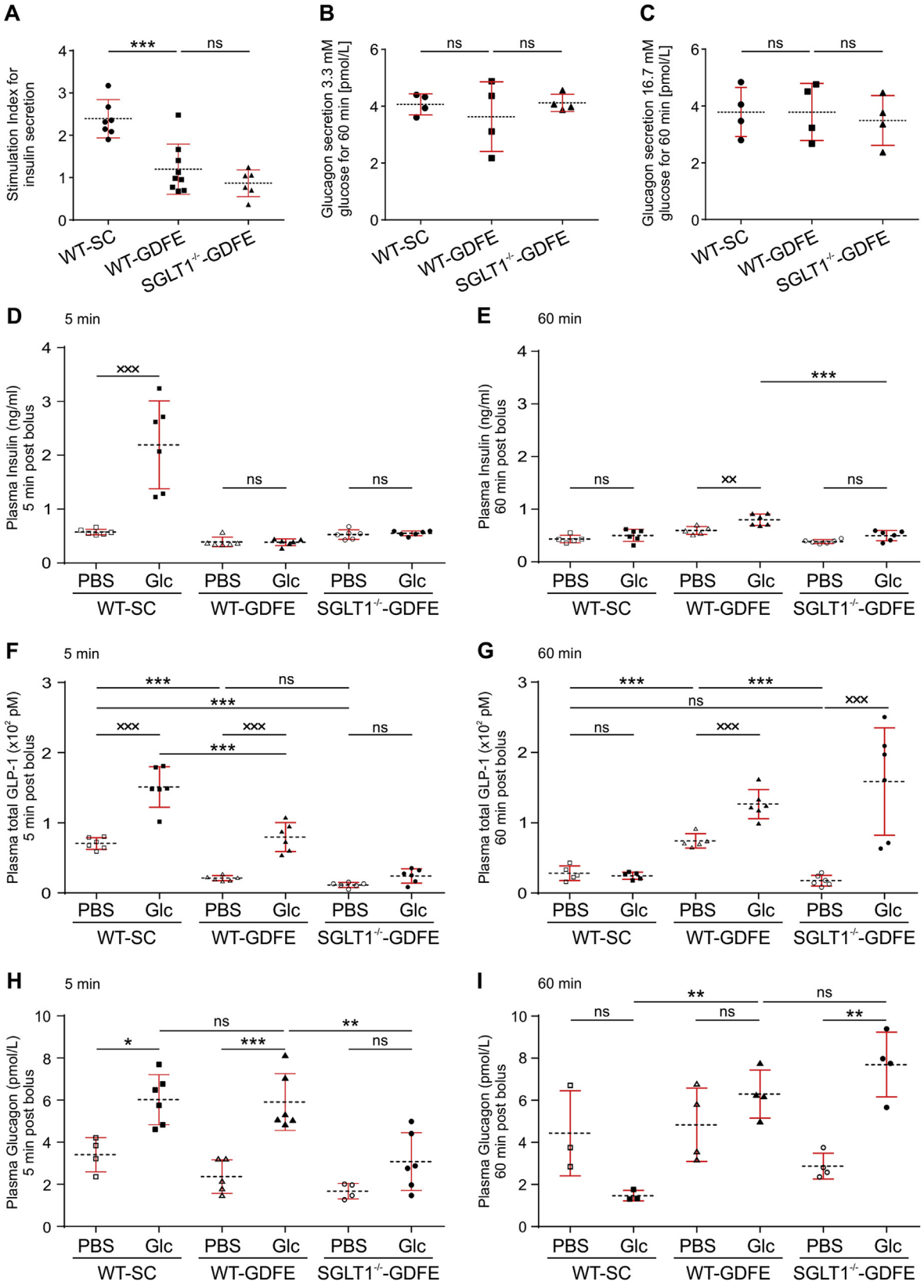

Figure 4: Glucose-stimulated insulin and glucagon secretion in isolated islets and analysis of Insulin, glucagon, and GLP-1 levels in blood of WT-SC, WT-GDFE, and SGLT1$^{-/-}$-GDFE mice after glucose administration. Isolated PIs were cultured in the presence of 3.3 mM D-glucose followed by incubation for 60 min at 3.3 mM (low glucose) or 16.7 mM D-glucose (high glucose). Insulin secretion capacity of islets is shown as stimulation index **(A)**. Glucagon levels are shown as absolute values **(B,C)**. Both insulin and glucagon values are normalized to islet DNA. $n = 4$. Individual measurements are indicated as means ± SD. Concentrations of insulin **(D,E)**,GLP-1 **(F,G)** and glucagon

 © 2018 The Authors. Published by Elsevier GmbH. This is an open access article under the CC BY-NC-ND license (http://creativecommons.org/licenses/by-nc-nd/4.0/).

GDFE and SGLT1$^{-/-}$-GDFE mice, we analyzed PIs for fat incorporation, as a fat-enriched diet was recently shown to contribute to diminished glucose dependent insulin secretion [30—32]. Studying triglyceride deposition within PIs were performed by Oil Red O histological stainings. While SGLT1$^{-/-}$-GDFE pancreata displayed a flabby texture in comparison to WT mice on either SC or GDFE-diet indicating possible enrichment in fat, no significant differences in all three groups were detected by the Oil Red O staining (Supplementary Fig. 6). Of note and further arguing against an increase in fat, body weight was not only significantly reduced in SGLT1$^{-/-}$-GDFE mice but also in WT-GDFE controls (Supplementary Fig. 6B).

3.5. SGLT1$^{-/-}$ mice on glucose-deficient, fat-enriched diet show altered blood insulin, glucagon, and GLP-1 levels

In order to investigate if the insulin or glucagon secretion capacity of PIs from WT-GDFE mice is compromised *in vivo*, we next performed an oral glucose tolerance test (OGTT). As intestinal GLP-1 secretion is an important regulatory mechanism for insulin secretion [33], which was previously shown to be impaired in SGLT1$^{-/-}$ mice [7,8] we also analyzed GLP-1 values in this work. Former studies revealed an impaired insulin and GLP-1 secretion in SGLT1$^{-/-}$-GDFE mice 5—15 min after glucose gavage [7,8]. In these studies, 2—3 months old SGLT1$^{-/-}$ mice on GDFE [7] were analyzed in comparison to either WT mice on SC [7] or GDFE applied for only one week [8]. Our study addresses a prolonged application of the GDFE-diet. We measured insulin and also GLP-1 levels after OGTT in the systemic blood comparing WT-GDFE and SGLT1$^{-/-}$-GDFE mice, both fed the same duration with GDFE-diet (Figure 4D—G). WT-SC mice served as additional control group. In WT-SC mice 5 min after glucose gavage, blood insulin concentration was increased 3.8-fold (Figure 4D) and decreased to the fasting level after 60 min (Figure 4E). This is in contrast to WT-GDFE animals with no significant increase of blood insulin 5 min after glucose gavage but up to 34% increase 60 min after glucose gavage (Figure 4D and E). In SGLT1$^{-/-}$-GDFE mice, no increase of blood insulin was observed 5 min and 60 min after glucose gavage (Figure 4D and E) demonstrating no insulin responses at both specific time points when SGLT1 is abrogated. Prompted by these findings, we next investigated if these observations are associated with a deregulation in GLP-1 secretion. Measurements of GLP-1 concentrations 5 min after glucose gavage showed increased blood GLP-1 levels by 80 $\pm$ 29 pMol and 58 $\pm$ 20 pMol in WT-SC and WT-GDFE mice (Figure 4F). In contrast, no significant increase of blood GLP-1 was observed in SGLT1$^{-/-}$-GDFE mice (Figure 4F). 60 min after glucose gavage, blood GLP-1 was not changed in WT-SC mice; however, it was increased by 52 $\pm$ 20 pMol in WT-GDFE mice and by 126 $\pm$ 62 pMol in SGLT1$^{-/-}$-GDFE mice ($P < 0.05$ for difference between WT-GDFE and SGLT1$^{-/-}$-GDFE mice) (Figure 4G). Analyses of glucagon levels (Figure 4H and I) revealed a significant increase in blood glucagon for WT-SC and WT-GDFE mice 5 min after glucose administration while SGLT1$^{-/-}$-GDFE mice showed no significantly elevated blood glucagon levels (Figure 4H). However, increased blood glucagon levels were demonstrated for SGLT1$^{-/-}$-GDFE mice 60 min after glucose administration (Figure 4I). While glucagon levels for WT-SC mice dropped off after 60 min, WT-GDFE animals displayed marginally elevated blood glucagon levels (Figure 4I).

4. DISCUSSION

SGLT1 is known to be predominantly expressed in the small intestine playing a leading role in intestinal glucose absorption. Here we demonstrate the downregulation of small intestinal SGLT1 under low glucose conditions. Corresponding to the reduced mRNA expression levels, SGLT1 function also was impaired. A nutrient-dependent regulation of SGLT1 was published recently [2,27,34]. In this context, Shirazi-Beechey et al. showed an upregulation of SGLT1 when glucose is high [27]. In summary, these data prove glucose to be an important regulator for small intestinal SGLT1 expression and function while the impact of the dietary fat remains elusive.

Apart from the small intestine, SGLT1 was recently shown to be expressed in various other organs like the pancreas [1—3,5,6,23,24]. Pancreatic SGLT1 mRNA was unaltered under diet conditions suggesting different regulatory mechanisms for SGLT1 in diverse tissues. SGLT1 mRNA expression was shown for PIs and the exocrine pancreas; however, at drastically reduced levels compared to the small intestine. The low expression levels could be explained by SGLT1 abundance only in cellular subsets of both pancreatic regions. While SGLT1 expression is described for all islet cell types except of β-cells, exocrine-specific expression was shown only for duct cells [3,6,23].

In light of pancreatic SGLT1 expression and due to a lack of knowledge about its function, we investigated if loss of SGLT1 impacts PIs. Our data provided evidence for an aberrant pancreatic islet morphology including enlarged sizes associated with elevated cell numbers but unchanged cellular densities. Further, apoptotic cell numbers were reduced explaining the increase in islet cell numbers and therefore size. In addition, the majority of SGLT1$^{-/-}$ islets displayed an atypical cytomorphology characterized by a decrease of the β- and increase of the α-cell proportion. Prolonged feeding of mice with GDFE also resulted in atypical islet cytomorphology. However, the proportion of α- and β-cells was not significantly altered in WT-GDFE mice, albeit marginal differences to WT-SC controls were observed. As SGLT1 expression was only reduced, but not completely abolished, in GDFE fed wild type mice, the remaining SGLT1 expression may account for these differences in effect strength between WT-GDFE and SGLT1$^{-/-}$ islets. In summary, our data hypothesize a role for SGLT1 maintaining typical islet (cyto)morphology including cellular composition of the islet. Mechanistically, these observations could rely on an impairment in glucose transport and/or sensing due to loss of SGLT1. Glucose is known to be of high importance for PIs, regulating β-cell survival and proliferation in an age- and dose-dependent manner [35,36]. Diminished survival and proliferation rates were demonstrated with decreasing glucose concentrations [35]. Further, elevated glucose levels are associated with increased islet cell apoptosis [37,38]. Loss of SGLT1 associated with an underrepresentation of postprandial blood glucose could therefore explain the impaired cellular proliferation and reduction in apoptotic cells. Given that SGLT1 expression was shown for diverse islet-specific cell types [3,6], loss of SGLT1 function could further result in aberrant glucose transport and/or sensing within the pancreatic islet. In this context, we hypothesize that the lack of SGLT1 function possibly promotes a rescue mechanism within the murine islet to cope with the unavailability of glucose by increasing the proportion of glucagon-secreting α-cells thereby driving gluconeogenesis.

(H,I) in systemic blood were analyzed 5 min **(D,F,H)** or 60 min **(E,G,I)** after gavage with phosphate buffered saline without glucose (PBS) or glucose (Glc) in WT-SC, WT-GDFE or SGLT1$^{-/-}$-GDFE animals ($n = 3$ - 6). The determinations of insulin, GLP-1 and glucagon were performed in duplicates. Islet stimulation and *in vivo* experiments were performed with male mice. Means $\pm$ SD and measurements from individual animals are indicated. *$P < 0.05$, **$P < 0.01$, ***$P < 0.001$, ns = not significant one-way ANOVA with posthoc Tukey test. $^{\times\times}P < 0.01$, $^{\times\times\times}P < 0.001$, ns = not significant Student's *t*-test.

 © 2018 The Authors. Published by Elsevier GmbH. This is an open access article under the CC BY-NC-ND license (http://creativecommons.org/licenses/by-nc-nd/4.0/).

To what extent intestinal or pancreatic SGLT1 function contribute needs to be addressed in future studies.

To date, a detailed understanding for the increase in α-cells is missing. As cellular plasticity was shown for pancreatic islet cells [39], one possible explanation would be the transdifferentiation of other islet cell types into α-cells but an exocrine origin also would be conceivable. SGLT1 expression was recently demonstrated within intralobular duct cells of the pancreas [6,23] but functional aspects remain unknown. Given that pancreatic duct cells represent progenitors for all endocrine cell types during development [40–42], it would be of great interest to know if loss of SGLT1 function is associated with a change in interstitial glucose concentration and if this affects islet morphology and/or cellular alterations already at early developmental stages. Future long-term studies are urgently needed to investigate if SGLT1 ablation is indeed associated with disturbed glucose transport and/or sensing possibly contributing to the onset, progression and/or manifestation of the altered (cyto)morphology observed in SGLT1$^{-/-}$ islets. In addition, using a conditional knockout mouse model specific for pancreatic islet cell types will highlight if intestinal or pancreatic SGLT1 accounts for the impact on PIs.

In addition to structural aspects, our data provided evidence for aberrant insulin responses of WT and SGLT1$^{-/-}$ mice on GDFE diet. Mechanistically, loss of SGLT1 and feeding GDFE diet results in lower blood glucose levels compared to wild type mice on standard chow and therefore a limitation of the main regulator for insulin secretion from pancreatic β-cells. This proposes a dysfunction of the intestine regarding its glucose absorbance capacity as an underlying mechanism for the attenuated insulin responses. However, glucose stimulation of isolated islets from WT-GDFE or SGLT1$^{-/-}$-GDFE mice demonstrated lower stimulation indexes compared to WT-SC mice, a finding that indicates an impaired functionality of the β-cell itself. A detailed knowledge about cellular or molecular reasons as well as physiological causes remains unknown and needs to be addressed in detail in future studies.

In the past, a direct relation between fat-enriched diets and impaired insulin responses was demonstrated [30–32,43]. As dietary fat is known to change lipid composition in islet cell membranes, therefore hindering glucose transport and/or glucose sensing [31], the fat component of the GDFE diet could explain our findings regarding the impaired or absent insulin responses. However, we could not detect the incorporation of fat within PIs or anywhere in the pancreas (see Fig. S6C). In conclusion, these data point to another mechanism that contributes to the decreased insulin secretion capacity of WT or SGLT1$^{-/-}$ mice on GDFE diet.

Along with the SGLT1-mediated glucose absorption, the secretion of GLP-1 from enteroendocrine L-cells is regulated within the intestine which further stimulates insulin-secretion from pancreatic β-cells in addition to glucose [9–11]. In line with recent publications, we demonstrate no GLP-1 response in SGLT1$^{-/-}$-GDFE mice 5 min after OGTT contributing to the missing rise in blood insulin in these animals at this time point. Furthermore, this finding underlines the importance of SGLT1 in the regulation of acute GLP-1 secretion [7,24,44]. In contrast to SGLT1$^{-/-}$ mice, WT-GDFE animals showed an acute GLP-1 secretion but also no insulin response. Despite the secretion of GLP-1, blood glucose levels that are too low or possibly dysfunctional β-cells in these mice most likely account for this observation.

Both GDFE-fed animal groups displayed a sustained release of GLP-1 measured 60 min after OGTT. Similar findings were recently observed for SGLT1$^{-/-}$ mice demonstrating the delivery of glucose to the more distal gut and thereby initiating the sustained release of GLP-1 when SGLT1 is absent [13,14,45]. The reduced expression of SGLT1 in WT-GDFE mice possibly explains the sustained release of GLP-1 in these mice, similar to what is observed in SGLT1$^{-/-}$ animals. The sustained release of GLP-1 also might explain recently published results that demonstrate a weak insulin response in SGLT1$^{-/-}$ mice 10 - 15 min after OGTT, a time point that was not analyzed in our study [7,8]. Together with our findings, these data suggest a delayed insulin response mainly triggered by sustained GLP-1 release in the absence of SGLT1. As the increase in blood insulin shown by recent studies was only marginal, an impairment or dysfunction of β-cells for insulin secretion is further supported. This dysfunction possibly arises during development and manifests throughout aging due to the low levels of blood glucose. As glucagon secreted from α-cells is known to counteract rising insulin levels in the blood, our data further indicate a dominant role for glucagon in the context of the impaired rise in blood insulin levels observed for WT-GDFE or SGLT1$^{-/-}$-GDFE mice. In both animal groups, increased glucagon levels could be detected compared to PBS controls 5 and 60 min after OGTT. Stimulation of glucagon release from α-cells in the absence of insulin can be triggered by hypoglycemia [46]. Possible mechanistic explanations include the control of glucagon secretion via effector molecules like Zn^{2+} [47], γ-aminobutyric acid [48] or somatostatin [49]. Further, neuronal regulated glucose sensing [50,51] or the hyperpolarization of the α-cell due to low blood glucose could play a role [52]. To what extent which of these possibilities contribute to our findings remains elusive.

5. CONCLUSION

In summary, loss or impairment of SGLT1 resulted in abnormal pancreatic islet (cyto)morphology and disturbed islet function in the context of insulin or glucagon secretion from β- or α-cells, respectively. As a result, our findings propose a new, additional role for SGLT1 in maintaining proper islet structure and function.

In view of the recently published positive impact of SGLT1 inhibition on postprandial blood glucose levels under healthy or diabetic conditions [7,8,14–16], our data further signify the urgent need of long-term studies to investigate possible tissue-specific side effects when SGLT1 function is lost or impaired.

AUTHOR CONTRIBUTIONS

M.Mü. and D.Z. designed the study, performed experiments, and wrote the manuscript and take full responsibility for the article and its originality. A.F. contributed to glucose-stimulation experiments and reviewed the manuscript. C.B. supported experimental analysis and reviewed the manuscript. C.O. and H.W. reviewed the manuscript and contributed to the discussion. H.K. supported study design and manuscript writing and provided the SGLT1$^{-/-}$ mice. M.Me. designed the study, reviewed the manuscript, and contributed to the discussion. All authors approved the final version of the manuscript.

FUNDING

This work was supported by grants of the “Bayern FIT Programm” of the Bavarian state government, Germany.

ACKNOWLEDGEMENTS

The authors thank Manuela Hoffmann from the Department of General Visceral Vascular and Pediatric Surgery, University Hospital Würzburg, Renate Bausch and Heike Oberwinkler from the Chair Tissue Engineering and Regenerative Medicine, University Hospital Würzburg for their excellent technical assistance.

 © 2018 The Authors. Published by Elsevier GmbH. This is an open access article under the CC BY-NC-ND license (http://creativecommons.org/licenses/by-nc-nd/4.0/).

CONFLICT OF INTEREST

None declared.

APPENDIX A. SUPPLEMENTARY DATA

Supplementary data related to this article can be found at https://doi.org/10.1016/j.molmet.2018.05.011.

REFERENCES

[1] Koepsell, H., 2017. The Na+-D-glucose cotransporters SGLT1 and SGLT2 are targets for the treatment of diabetes and cancer. Pharmacology and Therapeutics 170:148–165.

[2] Wright, E.M., Loo, D.D., Hirayama, B.A., 2011. Biology of human sodium glucose transporters. Physiological Reviews 91(2):733–794.

[3] Bonner, C., Kerr-Conte, J., Gmyr, V., Queniat, G., Moerman, E., Thevenet, J., et al., 2015. Inhibition of the glucose transporter SGLT2 with dapagliflozin in pancreatic alpha cells triggers glucagon secretion. Nature Medicine 21(5):512–517.

[4] Zhou, L., Cryan, E.V., D'Andrea, M.R., Belkowski, S., Conway, B.R., Demarest, K.T., 2003. Human cardiomyocytes express high level of Na+/glucose cotransporter 1 (SGLT1). Journal of Cellular Biochemistry 90(2):339–346.

[5] Salker, M.S., Singh, Y., Zeng, N., Chen, H., Zhang, S., Umbach, A.T., et al., 2017. Loss of endometrial sodium glucose cotransporter SGLT1 is detrimental to embryo survival and fetal growth in pregnancy. Scientific Reports 7(1):12612.

[6] Segerstolpe, A., Palasantza, A., Eliasson, P., Andersson, E.M., Andreasson, A.C., Sun, X., et al., 2016. Single-cell transcriptome profiling of human pancreatic islets in health and type 2 diabetes. Cell Metabolism 24(4):593–607.

[7] Gorboulev, V., Schurmann, A., Vallon, V., Kipp, H., Jaschke, A., Klessen, D., et al., 2012. Na(+)-D-glucose cotransporter SGLT1 is pivotal for intestinal glucose absorption and glucose-dependent incretin secretion. Diabetes 61(1):187–196.

[8] Roder, P.V., Geillinger, K.E., Zietek, T.S., Thorens, B., Koepsell, H., Daniel, H., 2014. The role of SGLT1 and GLUT2 in intestinal glucose transport and sensing. PLoS One 9(2):e89977.

[9] Deacon, C.F., Ahren, B., 2011. Physiology of incretins in health and disease. The Review of Diabetic Studies RDS 8(3):293–306.

[10] Drucker, D.J., 2013. Incretin action in the pancreas: potential promise, possible perils, and pathological pitfalls. Diabetes 62(10):3316–3323.

[11] Baggio, L.L., Drucker, D.J., 2007. Biology of incretins: GLP-1 and GIP. Gastroenterology 132(6):2131–2157.

[12] Martin, M.G., Turk, E., Lostao, M.P., Kerner, C., Wright, E.M., 1996. Defects in Na+/glucose cotransporter (SGLT1) trafficking and function cause glucose-galactose malabsorption. Nature Genetics 12(2):216–220.

[13] Oguma, T., Nakayama, K., Kuriyama, C., Matsushita, Y., Yoshida, K., Hikida, K., et al., 2015. Intestinal sodium glucose cotransporter 1 inhibition enhances glucagon-like Peptide-1 secretion in normal and diabetic rodents. Journal of Pharmacology and Experimental Therapeutics 354(3):279–289.

[14] Song, P., Onishi, A., Koepsell, H., Vallon, V., 2016. Sodium glucose cotransporter SGLT1 as a therapeutic target in diabetes mellitus. Expert Opinion on Therapeutic Targets 20(9):1109–1125.

[15] Shibazaki, T., Tomae, M., Ishikawa-Takemura, Y., Fushimi, N., Itoh, F., Yamada, M., et al., 2012. KGA-2727, a novel selective inhibitor of a high-affinity sodium glucose cotransporter (SGLT1), exhibits antidiabetic efficacy in rodent models. Journal of Pharmacology and Experimental Therapeutics 342(2):288–296.

[16] Dobbins, R.L., Greenway, F.L., Chen, L., Liu, Y., Breed, S.L., Andrews, S.M., et al., 2015. Selective sodium-dependent glucose transporter 1 inhibitors block glucose absorption and impair glucose-dependent insulinotropic peptide release. American Journal of Physiology Gastrointestinal and Liver Physiology 308(11):G946–G954.

[17] Sands, A.T., Zambrowicz, B.P., Rosenstock, J., Lapuerta, P., Bode, B.W., Garg, S.K., et al., 2015. Sotagliflozin, a dual SGLT1 and SGLT2 inhibitor, as adjunct therapy to insulin in type 1 diabetes. Diabetes Care 38(7):1181–1188.

[18] Zambrowicz, B., Freiman, J., Brown, P.M., Frazier, K.S., Turnage, A., Bronner, J., et al., 2012. LX4211, a dual SGLT1/SGLT2 inhibitor, improved glycemic control in patients with type 2 diabetes in a randomized, placebo-controlled trial. Clinical Pharmacology and Therapeutics 92(2):158–169.

[19] Turk, E., Martin, M.G., Wright, E.M., 1994. Structure of the human Na+/glucose cotransporter gene SGLT1. Journal of Biological Chemistry 269(21):15204–15209.

[20] Turk, E., Zabel, B., Mundlos, S., Dyer, J., Wright, E.M., 1991. Glucose/galactose malabsorption caused by a defect in the Na+/glucose cotransporter. Nature 350(6316):354–356.

[21] Li, D.S., Yuan, Y.H., Tu, H.J., Liang, Q.L., Dai, L.J., 2009. A protocol for islet isolation from mouse pancreas. Nature Protocols 4(11):1649–1652.

[22] Zmuda, E.J., Powell, C.A., Hai, T., 2011. A method for murine islet isolation and subcapsular kidney transplantation. Journal of visualized experiments JoVE(50).

[23] Madunic, I.V., Breljak, D., Karaica, D., Koepsell, H., Sabolic, I., 2017. Expression profiling and immunolocalization of Na+-D-glucose-cotransporter 1 in mice employing knockout mice as specificity control indicate novel locations and differences between mice and rats. Pfluegers Archiv European Journal of Physiology.

[24] Vrhovac, I., Balen Eror, D., Klessen, D., Burger, C., Breljak, D., Kraus, O., et al., 2015. Localizations of Na(+)-D-glucose cotransporters SGLT1 and SGLT2 in human kidney and of SGLT1 in human small intestine, liver, lung, and heart. Pfluegers Archiv European Journal of Physiology 467(9):1881–1898.

[25] Ferraris, R.P., 2001. Dietary and developmental regulation of intestinal sugar transport. Biochemical Journal 360(Pt 2):265–276.

[26] Drozdowski, L.A., Thomson, A.B.R., 2006. Intestinal sugar transport. World Journal of Gastroenterology 12(11):1657–1670.

[27] Shirazi-Beechey, S.P., Hirayama, B.A., Wang, Y., Scott, D., Smith, M.W., Wright, E.M., 1991. Ontogenic development of lamb intestinal sodium-glucose co-transporter is regulated by diet. Journal of Physiology 437:699–708.

[28] Jo, J., Hara, M., Ahlgren, U., Sorenson, R., Periwal, V., 2012. Mathematical models of pancreatic islet size distributions. Islets 4(1):10–19.

[29] Scholzen, T., Gerdes, J., 2000. The Ki-67 protein: from the known and the unknown. Journal of Cellular Physiology 182(3):311–322.

[30] Ahren, B., Gudbjartsson, T., Al-Amin, A.N., Martensson, H., Myrsen-Axcrona, U., Karlsson, S., et al., 1999. Islet perturbations in rats fed a high-fat diet. Pancreas 18(1):75–83.

[31] Lichtenstein, A.H., Schwab, U.S., 2000. Relationship of dietary fat to glucose metabolism. Atherosclerosis 150(2):227–243.

[32] Wang, Y., Miura, Y., Kaneko, T., Li, J., Qin, L.Q., Wang, P.Y., et al., 2002. Glucose intolerance induced by a high-fat/low-carbohydrate diet in rats effects of nonesterified fatty acids. Endocrine 17(3):185–191.

[33] MacDonald, P.E., El-Kholy, W., Riedel, M.J., Salapatek, A.M., Light, P.E., Wheeler, M.B., 2002. The multiple actions of GLP-1 on the process of glucose-stimulated insulin secretion. Diabetes 3(51 Suppl):S434–S442.

[34] Miyamoto, K., Hase, K., Takagi, T., Fujii, T., Taketani, Y., Minami, H., et al., 1993. Differential responses of intestinal glucose transporter mRNA transcripts to levels of dietary sugars. Biochemical Journal 295(Pt 1):211–215.

[35] Assefa, Z., Lavens, A., Steyaert, C., Stange, G., Martens, G.A., Ling, Z., et al., 2014. Glucose regulates rat beta cell number through age-dependent effects on beta cell survival and proliferation. PLoS One 9(1):e85174.

[36] Stamateris, R.E., Sharma, R.B., Kong, Y., Ebrahimpour, P., Panday, D., Ranganath, P., et al., 2016. Glucose induces mouse beta-cell proliferation via IRS2, MTOR, and cyclin D2 but not the insulin receptor. Diabetes 65(4):981–995.

 © 2018 The Authors. Published by Elsevier GmbH. This is an open access article under the CC BY-NC-ND license (http://creativecommons.org/licenses/by-nc-nd/4.0/).

[37] Maedler, K., Spinas, G.A., Lehmann, R., Sergeev, P., Weber, M., Fontana, A., et al., 2001. Glucose induces beta-cell apoptosis via upregulation of the Fas receptor in human islets. Diabetes 50(8):1683–1690.

[38] Cerf, M.E., 2013. Beta cell dysfunction and insulin resistance. Frontiers in Endocrinology 4:37.

[39] van der Meulen, T., Huising, M.O., 2015. Role of transcription factors in the transdifferentiation of pancreatic islet cells. Journal of Molecular Endocrinology 54(2):R103–R117.

[40] Herrera, P.L., Huarte, J., Sanvito, F., Meda, P., Orci, L., Vassalli, J.D., 1991. Embryogenesis of the murine endocrine pancreas; early expression of pancreatic polypeptide gene. Development 113(4):1257–1265.

[41] Mastracci, T.L., Sussel, L., 2012. The endocrine pancreas: insights into development, differentiation, and diabetes. Wiley Interdisciplinary Reviews Developmental Biology 1(5):609–628.

[42] Pictet, R.L., Clark, W.R., Williams, R.H., Rutter, W.J., 1972. An ultrastructural analysis of the developing embryonic pancreas. Developmental Biology 29(4): 436–467.

[43] Cerf, M.E., 2007. High fat diet modulation of glucose sensing in the beta-cell. Medical Science Monitor International Medical Journal of Experimental and Clinical Research 13(1):RA12–RA17.

[44] Reimann, F., Habib, A.M., Tolhurst, G., Parker, H.E., Rogers, G.J., Gribble, F.M., 2008. Glucose sensing in L cells: a primary cell study. Cell Metabolism 8(6):532–539.

[45] Tolhurst, G., Heffron, H., Lam, Y.S., Parker, H.E., Habib, A.M., Diakogiannaki, E., et al., 2012. Short-chain fatty acids stimulate glucagon-like Peptide-1 secretion via the g-protein-coupled receptor FFAR2. Diabetes 61(2): 364–371.

[46] Gylfe, E., 2013. Glucose control of glucagon secretion: there is more to it than KATP channels. Diabetes 62(5):1391–1393.

[47] Ishihara, H., Maechler, P., Gjinovci, A., Herrera, P.L., Wollheim, C.B., 2003. Islet beta-cell secretion determines glucagon release from neighbouring alpha-cells. Nature Cell Biology 5(4):330–335.

[48] Rorsman, P., Berggren, P.O., Bokvist, K., Ericson, H., Mohler, H., Ostenson, C.G., et al., 1989. Glucose-inhibition of glucagon secretion involves activation of GABAA-receptor chloride channels. Nature 341(6239):233–236.

[49] Starke, A., Imamura, T., Unger, R.H., 1987. Relationship of glucagon suppression by insulin and somatostatin to the ambient glucose concentration. Journal of Clinical Investigation 79(1):20–24.

[50] Miki, T., Liss, B., Minami, K., Shiuchi, T., Saraya, A., Kashima, Y., et al., 2001. ATP-sensitive K+ channels in the hypothalamus are essential for the maintenance of glucose homeostasis. Nature Neuroscience 4(5):507–512.

[51] Thorens, B., 2011. Brain glucose sensing and neural regulation of insulin and glucagon secretion. Diabetes Obesity and Metabolism 1(13 Suppl):82–88.

[52] Rorsman, P., Salehi, S.A., Abdulkader, F., Braun, M., MacDonald, P.E., 2008. K(ATP)-channels and glucose-regulated glucagon secretion. Trends in Endocrinology and Metabolism 19(8):277–284.

 © 2018 The Authors. Published by Elsevier GmbH. This is an open access article under the CC BY-NC-ND license (http://creativecommons.org/licenses/by-nc-nd/4.0/).